EFFECT OF LASER WELDING ON SAFETY CHARACTERISTICS OF HIGH STRENGTH STEELS SHEETS

Emil Evin[1)], Stanislav Németh[1)], Miroslav Tomáš[1)]*
[1)] *Technical University of Košice, Faculty of Mechanical Engineering, Košice, Slovakia*

Received: 20.08.2015
Accepted: 13.09.2015

[*]*Corresponding author: emil.evin@tuke.sk, tel.: +421 55 602 3547, Department of Automotive Production, Faculty of Mechanical Engineering, Technical University of Košice, Letná 9, 04200 Košice, Slovakia*

Abstract
In the automotive industry considerable attention is paid to innovations oriented especially to meeting safety and environmental requirements. Concepts of vehicle safety focus on resistance of deformation zone components to impact and resistance to intrusion of undesirable fragments into the passengers´ space. In terms of these aspects the samples of the base materials from micro-alloyed steels HSLA - H220PD, DP 600 and TRIP - RAK 40/70 and also welded by solid-state fibre laser YLS-5000 were analysed. Multi-phase structure materials TRIP - RAK 40/70 and DP 600 showed considerably higher values of absorption capacity, strength, and stiffness than in case of single-phase structure material HSLA - H220PD. The greatest values of absorption capacity, strength, and stiffness were recorded in material TRIP - RAK 40/70 with ferritic matrix and a certain fraction of residual austenite, bainite, and martensite. Absorption capacity, strength, and stiffness have strong correlation with material constant K and strain hardening exponent.

Keywords: laser welding, tensile test, TRIP, HSLA, mechanical properties

1 Introduction

The lifetime assessment and potential for possible failure of in-service components is acritical issue in the safety and reliability analysis of components and products in consumer and automotive industry [1]. Nowadays, the pace of implementation of more radical changes (innovations) in the automotive industry has been being increased, so the lifetime of car body components and the whole car is increased as well. The main intention is to provide the customer with independent information on vehicle´s safety and to enable producers to obtain information on distinction of their automobiles from those of the competitors on the basis of test such as frontal and side-impact, pole-impact and roof landing tests, and thus to increase competitiveness of their vehicles [2].

In case of the external compatibility of safety requirements, it is about matching deformation forces and deformation travels with regard to distribution of the impact (absorbed) energy of all persons involved in an accident, keeping biomechanical limit values, and maintaining the space for survival. Measures for ensuring internal and external safety serve for providing all road traffic participants with the greatest possible hope for survival in case of an accident and for making the risk of injury as low as possible [3].

DOI 10.12776/ams.v21i3.603 p-ISSN 1335-1532
e-ISSN 1338-1156

Homologation regulations do not specify directly structural solutions of deformation zone components and materials of the deformation zone components, but for crash the guarantee of prescribed effects or safety characteristics is required.

Safety requirements and reducing of weight and emissions have put great pressure on development of new types of materials (high-strength steels, aluminium alloys, plastics as composite materials etc.) and non-traditional manufacturing processes (tailored welded blanks, hydroforming methods, forming using gaseous media etc.). Non-traditional processes of production of components of mechanical systems of vehicles´ passive safety may have a different impact on safety characteristics of components in static or dynamic loading by tension, compression, bending, torsion, shear than conventional methods.

When designing a car body structure, designers need information on strength and deformation characteristics of new materials and also on impact of used technologies to those characteristics. Safety characteristics of deformation zone components are related in most cases to deformation work – toughness, strength, stiffness, fatigue etc. [4, 5]

An important and challenging issue in the automotive industry is lightweight, safe design and enhancement of the crash response of auto-body structures. The most widely-used automotive steels are interstitial free steel, micro-alloyed steel, dual phase and transformation induced plasticity steels [5, 6, 7]. Dual-phase steels have a microstructure which contains predominately martensite (there can be small amounts of retained austenite, bainite or pearlite) in a ferrite matrix, and these steels exhibit characteristic mechanical properties, i.e. continuous yielding, a high tensile strength to yield strength ratio, and very high initial work hardening rates. The combination of high strength and high ductility has made DP steels very attractive to industry, particularly to the automobile sector. [5, 8, 9].

2 Experimental Materials and Methods

In experimental research of laser-beam welding impact on safety characteristics of components of deformation zones of passengers (cabin), plates from micro-alloyed steel HSLA - H220PD, from multi-phase steels DP 600 and TRIPRAK 40/70, whose chemical composition (tab. 1) was defined by the mobile spectrometer Belec Compact Port, were used.

Table 1 Chemical composition of materials used

Material	**Chemical composition [%]**								
HSLA H220PD	C	Si	Mn	P	S	Cu	Al	Cr	Mo
	<0.077	0.019	0.358	0.011	<0.002	0.017	0.026	0.009	<0.007
	Ni	V	Ti	Nb	Co	W	Fe		
	<0.002	0.003	<0.002	0.031	0.017	<0.036	99.38		
DP 600	C	Si	Mn	P	S	Cu	Al	Cr	Mo
	<0.111	0.279	1.963	0.026	<0.002	0.019	0.031	0.206	<0.002
	Ni	V	Ti	Nb	Co	W	Fe		
	<0.002	0.012	<0.002	0.02	0.017	<0.005	97.31		
TRIP - RAK 40/70	C	Si	Mn	P	S	Cu	Al	Cr	Mo
	<0.089	0.182	1.591	0.028	<0.002	0.023	2,267	0.042	0.022
	Ni	V	Ti	Nb	Co	W	Fe		
	<0.002	0.011	<0.007	0.022	0.022	<0.002	9569		

DOI 10.12776/ams.v21i3.603 p-ISSN 1335-1532
e-ISSN 1338-1156

Blanks from plates of micro-alloyed steel HSLA - H220PD, from multi-phase steels DP 600 and TRIP steel RAK 40/70 were welded by means of continuous welding (CW) without protecting gas by solid-state fibre laser YLS-5000 from the company called IPG Laser. Laser welding modes applied are stated in table 2. [10]

Basic mechanical properties like yield strength Re, tensile strength, uniform ductility till neck formation (necking), ductility, material constant K, exponent of strain hardening of the examined basic materials and laser-welded blanks were found out by standardised tests in accordance with STN EN 10 002-1, ISO 10113:2006 and ISO 10275:2007 with the sample stated in Fig. 1 and Fig. 2 from load diagrams of the tensile testing machine TIRATEST 2300 measured at the strain rate $\dot{\varepsilon} = \varepsilon/t = 0.0021\ s^{-1}$.

Table 2 Laser welding parameters

Sample	Thickness of sheet [mm]	Output of laser [W]	Focus position [mm]	Welding speed [mm.s^{-1}]	Note
HSLA H220PD	0,7	1,7	10	50	OK
		2,1		70	
		2,3		70	
DP600	0,7	2,0	10	50	OK
		2,7		70	
TRIP RAK 40/70	0,7	1,7	10	50	OK
		2,1		70	
		2,6		70	

*OK – best settings for laser welding

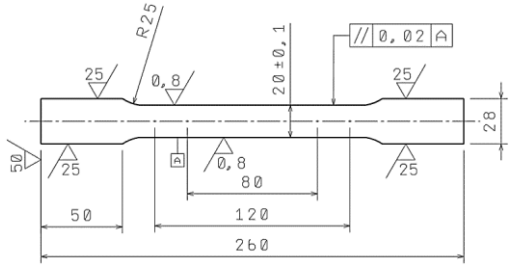

Fig. 1 Standardised sample for tensile test

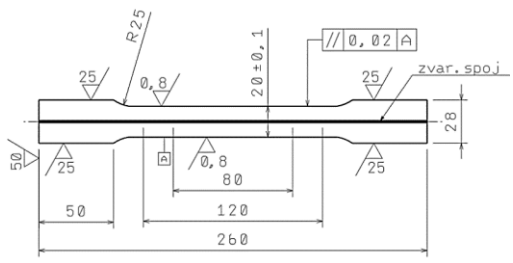

Fig. 2 Laser-welded sample

3 Results

Determining of carbon equivalent according to the relation (1.) is one of the options of complex assessment of welding property of non-alloy, micro-alloy, and medium-alloy steels to castings.

$$C_E = C + \frac{Mn}{6} + \frac{Cr}{5} + \frac{Ni}{15} + \frac{Mo}{4} + \frac{Cu}{13} + \frac{P}{2} + 0.0024 \cdot a_0 \qquad [\text{wgt\%}] \qquad (1.)$$

The equation (1.) applies to materials with the elements content up to: C <= 0.22 wgt%, Mn<= 1.6 wgt%, Cr <= 1 wgt%, Ni <= 3.0 wgt%, V =< 0.14 wgt%, Cu =< 0.30 wgt% [2, 4]. If Ce ≤ 0.50, then steel may be welded without any special measures. Then it results from **Tab. 1** that

DOI 10.12776/ams.v21i3.603 p-ISSN 1335-1532
e-ISSN 1338-1156

sheet blanks of HSLA - H220PD and TRIP - RAK 40/70 thick 0.75 mm and of DP 600 thick 0.75 mm can be welded under no special measures – they are weldable without fail.
For analysis of a weld joint macrostructure, base material (BM) microstructure, heat-affected zone (HAZ) microstructure, and weld metal (WM) microstructure there were samples taken for each welding mode applied. The visual inspection of the images of the microstructure and macrostructures did not detect pores and cracks in welds, and the weld roots were sufficiently penetrated.
It results from the stated that in the applied modes of the laser-beam welding the weld´s best quality was reached at lower speeds and smaller output. This finding is in accordance with the results [11, 12].
It can be seen from the analysis of images of the microstructure of the base material HSLA - H220PD that it is the question of the fine-grained ferritic structure. In the base material microstructure the secondary carbide and nitride additions are present – **Fig. 3a**.

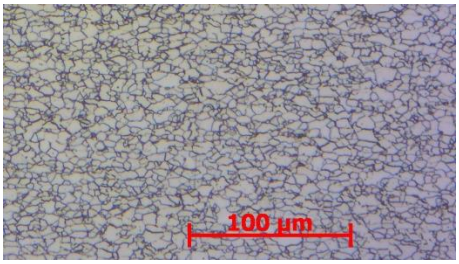

a)
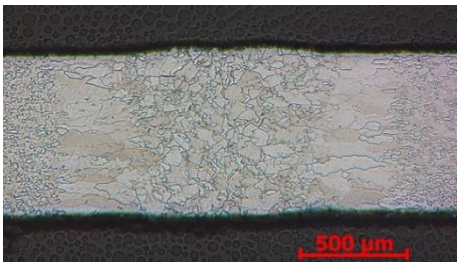

b)

Fig. 3 Microstructure of HSLA - H220PD a) base material, b) weld joint

The weld metal macrostructure consists of hypo-eutectoid ferrite which has been formed on the original austenitic grain boundaries, while the inside of the original austenitic grains is formed by fine acicular ferrite. In the microstructure of the basic metal also areas with the bainitic structure were observed. The structure of the weld metal as well as of the heat-affected zone is polyhedral and the grain size is greater in the heat-affected zone – Fig. 3b. Mechanical properties of base material and laser welded ones of HSLA steel are shown in **Table 3**.

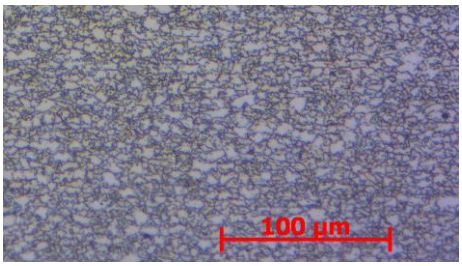

a)
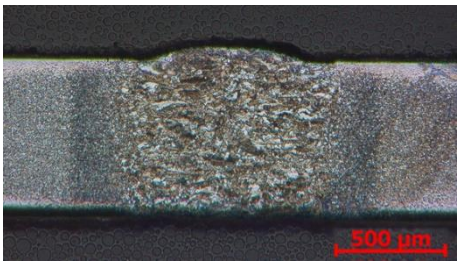

b)

Fig. 4 Microstructure of DP 600 a) base material, b) weld joint

It can be seen from the image (**Fig. 4a**) of the microstructure of the base material DP 600 that it is the ferritic-martensitic dual-phase steel with the ferrite-martensite ratio of about 70:30. From the macroscopic analysis of the DP 600 material samples (**Fig. 4b**) it can be seen that the weld metal as well as the heat-affected zone have a heterogeneous structure, while the heterogeneity is more significant in the weld metal. The heat-affected zone´s microstructure is formed by very

DOI 10.12776/ams.v21i3.603 p-ISSN 1335-1532
e-ISSN 1338-1156

fine martensite. Ferrite in a form of white blocks was observed especially on the boundary of the heat-affected zone and the base material. The weld metal microstructure is heterogeneous, formed by larger martensitic plates. Mechanical properties of base material and laser welded ones of DP 600 steel are shown in **Table 3**.

From the image (**Fig. 5a**) of the microstructure of the base material TRIP - RAK 40/70 it can be seen that the base is formed by a ferritic matrix in which there is a certain fraction of residual austenite, bainite, and martensite. The weld metal microstructure is heterogeneous, formed by residual austenite, upper bainite, martensite, and polyhedral ferritic grains (ferrite fraction of about 30%). Also the heat-affected zone is heterogeneous, formed by bainite and ferrite. The grain size increases in the direction towards the weld centre – **Fig. 5b**. Mechanical properties of base material and laser welded ones of TRIP steel are shown in Table 3. [10]

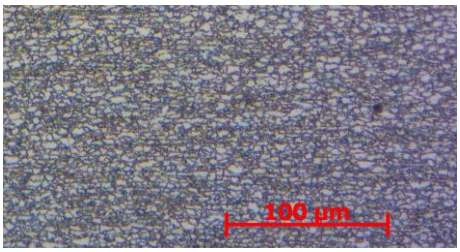

a)

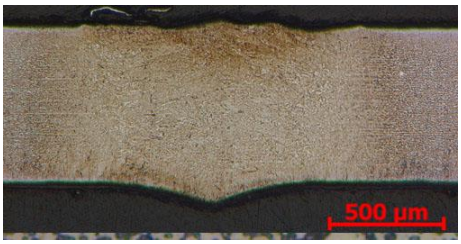

b)

Fig. 5 Microstructure of TRIP steel a) base material, b) weld joint

Table 3 Material properties of used steel sheets

Material		**Direction/ STDEV**	**$R_{P0,2}$ [MPa]**	**Rm [Mpa]**	**Ag [%]**	**A_{80} [%]**	**Ag_S [%]**	**K0,05 [MPa]**	**n0,05 [-]**	**r [-]**
HSLA H220PD	BM	90	388	449	17	29	24.9	728	0.179	0.659
	LWM	90	366	462	17	26	15.5	733	0.167	0.753
DP600	BM	90	376	632	19	28	24.8	1096	0.201	0.766
	LWM	90	435	677	17	20	16.2	1110	0.182	0.760
TRIP RAK 40/70	BM	90	440	764	24.8	29.9	26.4	1497	0.295	0.658
	LWM	90	466	657	20	21	18.1	1459	0.249	0.660

4 Discussion

In the automotive industry, there are two basic concepts of automobile safety. The first concept relates to impact resistance and the other one relates to resistance against intrusion of undesirable fragments into the passengers´ space.

Resistance to impact of deformation structure components is defined as a capability to absorb the impact energy using the mode of controlled failure of deformation zone components by gradual decomposition of energy in the profile at impact [13, 14].

So, the impact resistance depends on the absorption capability = toughness = strain energy ($W_{pl,necking}$ – Energy Absorbing) and expresses the material´s resistance against elastic and plastic deformation in various stress-strain schemes. Plastic deformation energy at uniaxial tension load can be expressed:

DOI 10.12776/ams.v21i3.603 p-ISSN 1335-1532
e-ISSN 1338-1156

a) by the area under the stress-strain curve in the engineering diagram using the engineering values of yield strength – Re, tensile strength – Rm, and total deformation - $\varepsilon_{max,c}$ – Fig. 6, when resistance of the material with a deformation grade decreases (necking) [15, 16].

$$W_{pl,necking} = \int_0^{dlmax} F \cdot dl \tag{2.}$$

If the force is expressed depending of the "mean stress value" calculated from the original cross-section of the sample S_0, yield strength, tensile strength

$$F = \frac{Re + Rm}{2} \cdot S_0 \tag{3.}$$

and the relative value of the maximum value of deformation $\varepsilon_{max,r}$

$$\varepsilon_{max,r} = \frac{dl_{max,r}}{L_0} \tag{4.}$$

then after the substitution and conversion the strain energy will be as follows:

$$W_{pl,necking} = \frac{Re + Rm}{2} \cdot S_0 \cdot L_0 \cdot \varepsilon_{max,necking} = \frac{Re + Rm}{2} \cdot V_0 \cdot \varepsilon_{max,necking} \tag{5.}$$

b) by the area under the curve true stress – true strain. For the numerical description of stress-strain curve Hollomon equation is commonly used in the following form [17]

$$\sigma = K \cdot \varphi^n \tag{6.}$$

and the true strain

$$\varphi = \ln \frac{L_0 + dl}{L_0} = \ln(1 + \varepsilon) \tag{7.}$$

then the true strain energy will be as follows:

$$W_{pl,necking} = \int_{0.002}^{\varphi_{max,necking}} K \cdot \varphi^n d\varphi \tag{8.}$$

and after integration and conversion we will reach:

$$W_{pl} = \frac{K \cdot S_0 \cdot L_0 \cdot \left(\varphi_{max,necking} - \varphi_{0.002}\right)^{n+1}}{n+1} \tag{9.}$$

Energy absorption capability of individual base materials and of laser-beam welded materials at impact was compared on the basis of strain energies calculated from the engineering diagram (using the relation 5) and true stress-strain diagram at maximum deformation and at 15% deformation (using the relation 9). As **Fig. 6** shows that from the engineering diagram it is difficult to define the maximum value of deformation at which the material is still able to absorb

DOI 10.12776/ams.v21i3.603 p-ISSN 1335-1532
e-ISSN 1338-1156

energy to necking (without failure), as in most materials the loading force or the engineering value of the tensile strength Rm oscillates at about the maximum value in greater range of deformations. Then the material´s capability to absorb energy depending on deformation to necking is determined by a drop of material´s resistance against plastic deformation in actual load diagram "actual stresses-deformation" and also the value of deformation $\varphi_{max,necking}$ corresponds to that.

Fig. 7 compares calculated strain energy necessary for deformation of samples of examined base materials and those laser-beam welded ones which were calculated according to the relation (5) and relation (9). Values of strain energy (absorbing capability), calculated according to relation (5), are in case of HSLA - H220PD material by 30 Nmm lower than according to the relation (9). A similar trend was also recorded with DP 600 material where the difference was 62 Nmm and with TRIP - RAK 40/70 material the difference was 69 Nmm.

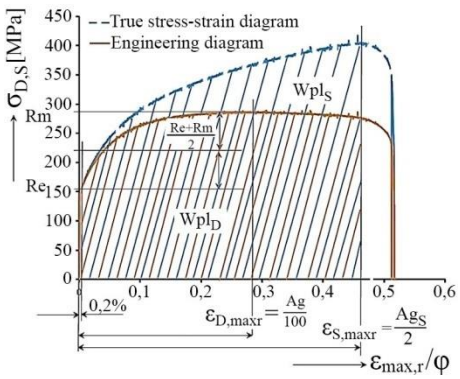

Fig. 6 Comparison of absorbing capacity calculated from engineering and true stress-strain diagram

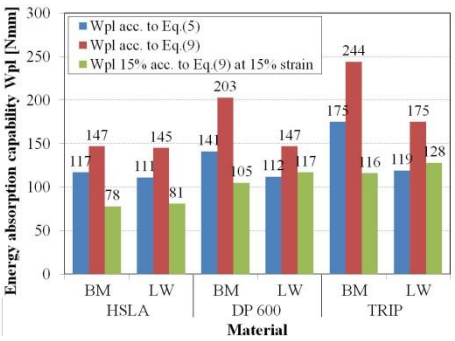

Fig. 7 Comparison of absorption capacity of experimental materials used (BM – base material, LW – laser welded material)

Impact of laser-beam welding has been shown more significantly in materials with multi-phase structure: DP 600 (BM 203 Nmm, LW 147 Nmm) and TRIP - RAK 40/70 (BM 244 Nmm, LW 175 Nmm) than in micro-alloyed steelHSLA - H220PD (BM 147 Nmm, LW 145 Nmm).

The second concept of resistance to penetration relates to absorption of impact energy without a possibility of penetration of a projectile or fragment into space for passengers with defined deformation of components or with their defined displacement [13, 14].

For example, for a crash it is required that in crash there may be no greater deformation of the deformation zone components than 15% and the required absorption energy must be min. 100 Nmm. Otherwise, there is a great risk of undesirable displacement and reduction of space for survival of the passengers. In such case, a principle should be observed that the difference between the total energy under the stress-strain curve before necking and the energy necessary for 15% deformation should not be little because there can appear a component failure much earlier than the required absorption energy is reached or there can appear larger displacement than required.

Our comparison of the absorbing capability of the examined material is based on the assumption that the absorption energy of 100Nmm and the maximum deformation ≤ 15% are required. Components made of HSLA - H220PD base material and also laser-beam welded despite the

DOI 10.12776/ams.v21i3.603 p-ISSN 1335-1532
e-ISSN 1338-1156

fact that their total capability of energy absorption is greater than 147 Nmm or 145 Nmm would not meet this condition as in an accident there would be greater displacement and reduction of the space for passengers´ survival. Components made of the base materials DP 600 and TRIP - RAK 40/70 but also laser-beam welded at 15% deformation are able to absorb the energy of 100 Nmm and they have a sufficient margin to avoid undesirable deformation of the deformation zone components and reduction of the space for passengers. In general it can be stated that the absorbing capacity of materials depends on ductility, strength, and stiffness.

Strength can be characterised as resistance of materials to formation of plastic deformation. In an accident, in the passengers´ zone there may be no penetration of any automobile´s fragments into the space for passengers and only little plastic deformation of the components or displacement is permissible.

If the assumption is that there may be no deformation, then the permissible tensile stress or strength can be expressed as a ratio of yield strength $R_{p0.2}$ to safety margin k for tough materials:

$$\sigma_{dov,t} = \frac{R_{P0.2}}{k} = \sigma_{el} \tag{10.}$$

and for brittle materials as a ration of tensile strength Rm to the safety margin k:

$$\sigma_{dov,t} = \frac{Rm}{k} = \sigma_{el} \tag{11.}$$

Stiffness can be expressed as an amount of elastic energy (W_{el} - EA) that can be absorbed by material at certain load within the area of purely elastic deformation (for example: ε_{el} 0.005% L0) per volume unit

$$W_{el} = F \cdot \chi_{\varepsilon<0.005} = \frac{R_{P0.2} \cdot S_0 \cdot L_0}{E \cdot k} \tag{12.}$$

where $R_{p0.005}$ is the elastic limit, the stress at the elastic limit will cause plastic deformation of less than 0.005% L0 and it results from the Hooke´s law that $\sigma_{el} = E.\varepsilon_{el}$. [18]

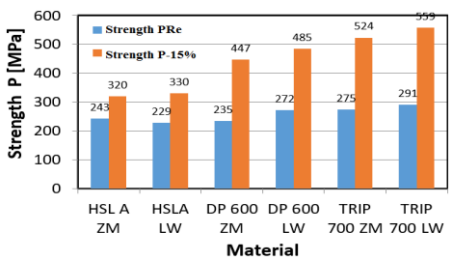

Fig. 8 Comparison of strength of examined materials

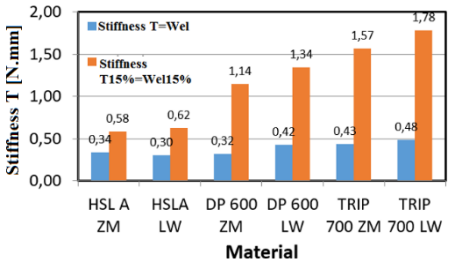

Fig. 9 Comparison of stiffness of examined materials

It results from **Fig. 8** and **9** that due to the impact of strain hardening at 15% deformation strength and stiffness of the deformation zone components will be increased. Greater gain in strength and stiffness was recorded in materials with multi-phase structure DP 600 and TRIP - RAK than in material with a single-phase structure HSLA - H220PD. The greatest values of the

absorbing capacity, strength, and stiffness were recorded in material TRIP - RAK 40/70 with the ferritic matrix and with a certain fraction of residual austenite, bainite, and martensite, because due to phase transformation of the residual austenite during deformation there is hardening taking place.

Based on the achieved results, former considerations and disscusion the following outputs can be drawn:

1. For experimental research, materials HSLA - H220PD, TRIP - RAK 40/70, and DP600 were used. Based on the carbon equivalent, steels HSLA - H220PD, TRIP - RAK 40/70 and DP can be welded without any special measures – they are weldable without fail. The microscopic and macroscopic analyses proved the assumption because pores and cracks in the welds were not found and the weld roots were sufficiently penetrated. The microstructure of the base material of HSLA - H220PD consists of hypo-eutectoid ferrite and secondary carbide and nitride additions. The structure of the base material of DP600 is a dual phase, ferrite-martensite structure with the volume fraction of ferrite 70% and martensite 30%. TRIP material is a three-phase steel of which the BM microstructure consists of ferrite, bainite, and residual austenite.
2. The microstructure of HSLA - H220PD weld metal consists of hypo-eutectoid ferrite and bainite. The structure of the weld metal and heat-affected zone of DP 600 is heterogeneous. The heat-affected zone microstructure consists of extra-fine martensite and the weld metal microstructure consists of larger martensite plates. The microstructure of the heat-affected zone of the material TRIP - RAK 40/70 is heterogeneous too, and is formed of bainite and ferrite. The weld metal microstructure consists of residual austenite, upper bainite, martensite, and ferrite (ferrite fraction of about 30%).
3. The total absorbing energy at the moment when there was a drop in material´s resistance to plastic deformation (necking) was assessed upon the engineering diagram and the true stress-strain diagram of the dependence of stress on strain. The absorbing capability values calculated from the engineering diagram are lower than the values calculated from the true stress-strain diagram. For assessment of the absorbing capacity we recommend to use the true stress-strain diagram, as it enables to express the impact of a grain size, impurities, various phases, deformation rate, temperature, etc. on deformation process. Because of deformation the material reaches greater resistance to plastic deformation, higher strength, hardness, lower ductility, and its other properties change as well.
4. In case that certain deformation (for example, deformation zones within the door area) or displacement are permissible, the absorbing capability of examined materials was compared by using the strain energy $W_{el\ 15\%}$ at 15% deformation. Also in this case, higher values of the absorbing capacity of materials with multi-phase structure DP 600 and TRIP - RAK 40/70 were recorded in comparison to the material HSLA - H220PD with a single-phase structure.
5. Materials with multi-phase structure TRIP - RAK 40/70 and DP 600 showed considerably higher values of the absorbing capacity, strength and stiffness than the material HSLA - H220PD with a single-phase structure. The highest values of the absorbing capacity, strength and stiffness were recorded in the material TRIP - RAK 40/70 with the ferritic matrix and a certain fraction of residual austenite, bainite and martensite, because due to phase transformation of residual austenite during deformation the hardening takes place.
6. The absorbing capacity, strength and stiffness have a strong correlation with the material constant K and the strain hardening exponent; and this is also the reason why multi-phase

DOI 10.12776/ams.v21i3.603 p-ISSN 1335-1532
e-ISSN 1338-1156

steels DP 600 and TRIP - RAK 40/70 show better absorbing capacity, strength and stiffness than micro-alloyed steel HSLA - H220PD.

5 Conclusion

The approach presented in the paper takes into account the basic material parameters to calculate safety characteristics of the material and influence of the laser welding to these characteristics. As presented in the paper, steels used show good weldability by laser welding without protective gas and any special measures. Laser welding do not influence significantly the strength, stiffness and absorbing capacity of steels; the higher values present materials with multi-phase structure – dual phase and Trip steels. The better absorbing capability also shows these steels when low permissible displacement of structural components is allowed (deformation zones within the door area). The total absorbing capacity is better to evaluate from the true stress-strain diagram of the dependence of stress on strain, as it enables to express the impact of material and loading parameters on deformation process.

The increasing safety requirements in cars require higher strength material to be used in critical safety elements in the car body. The increased use of AHSS is leading the way in crash safety. These steels provide an excellent way to reduce weight and improve performance, so they appear to be very attractive solutions for structural and safety parts of the car body.

References

[1] K. Matocha, L. Kander, M. Filip, O. Dorazil, K. Guan, Y. Xu: Acta Metallurgica Slovaca, Vol. 20, 2014, No. 4, p. 389-396, doi: 10.12776/ams.v20i4.425

[2] E. Incerti, A. Walker, J. Purton: *Trends in vehicle body construction and the potential implications for the motor insurance and repair industries*. In: International Bodyshop Industry Symposium, Montreux, Switzerland, 2005, p. 1-9

[3] U. Seiffwert, L. Wech: *Automotive Safety Handbook*, 1st ed., SAE International, 2003

[4] R. Kuziak, R. Kawalla, S. Waengler: Archives of Civil and Mechanical Engineering, Vol. 8, 2008, No. 2, p. 103-117

[5] N. Baluch, Z. M. Udin, Ch. S. Abdullah: Engineering, Technology & Applied Science Research, Vol. 4, 2014, No. 4, p. 686-689, doi: 10.5281/zenodo.14686

[6] H. Huh et al.: International Journal of Automotive Technology, Vol. 10, 2009, No. 2, p. 195-204, doi: 10.1007/s12239-009-0023-3

[7] L. Nemethova et al.: Acta Metallurgica Slovaca, Vol. 16, 2010, No. 2, p. 102-108

[8] M. Német, M. Mihaliková: Acta Polytechnica, Vol. 53, 2013, No. 4, p. 384-387

[9] M. Mihaliková, M. Német, V. Girman: Metalurgija. Vol. 54, 2015, No. 1, p. 211-213

[10] E. Evin, M. Kasenčák: Zvarac professional, Vol. 11, 2014, No. 1, p. 13-23, (in Slovak)

[11] Ch. Zhang et all.: Materials & Design, Vol. 36, 2012, p. 233-242, doi:10.1016/j.matdes.2011.11.016

[12] L. Mujica et all.: Materials Science and Engineering: A. Vol. 527, 2010, No. 7-8, p. 2071-2078, doi:10.1016/j.msea.2009.11.050

[13] G. C. Jacob, J. F. Fellers, S. Simunovic, J. M. Starbuck: Journal of Composite Materials, Vol. 36, 2002, No. 7, p. 813-580, doi: 10.1177/0021998302036007164

[14] W. J. Witteman: *Improved Vehicle Crash worthiness Design by Control of the Energy Absorption for Different Collision Situations*, 1st ed., Eindhoven University of Technology, 1999, ISBN 90-386-0880-2

[15] E. Evin et al.: Procedia Engineering, Vol. 69, 2014, p. 758-767, doi:10.1016/j.proeng.2014.03.052
[16] E. Evin, M. Tomáš: Procedia Engineering, Vol. 48, 2012, p. 115-122, doi:10.1016/j.proeng.2012.09.493
[17] A. Kováčová, T. Kvačkaj, R. Kočiško, J. Tiža: Acta Metallurgica Slovaca. Vol. 20, 2014, No. 3, p. 279-286, doi: 10.12776/ams.v20i3.359
[18] E. Evin et al: *Design of dual phase high strength steel sheets for autobody*. In: DAAAM International Scientific Book 2013, Vienna DAAAM International, p. 767-786, ISBN 978-3-901509-94-0, doi: 10.2507/daaam.scibook.2013.46

Acknowledgements
The contribution was working out with the support of the grant project VEGA 1/0824/12 and project APVV-0273-12.